

Supplementary Information

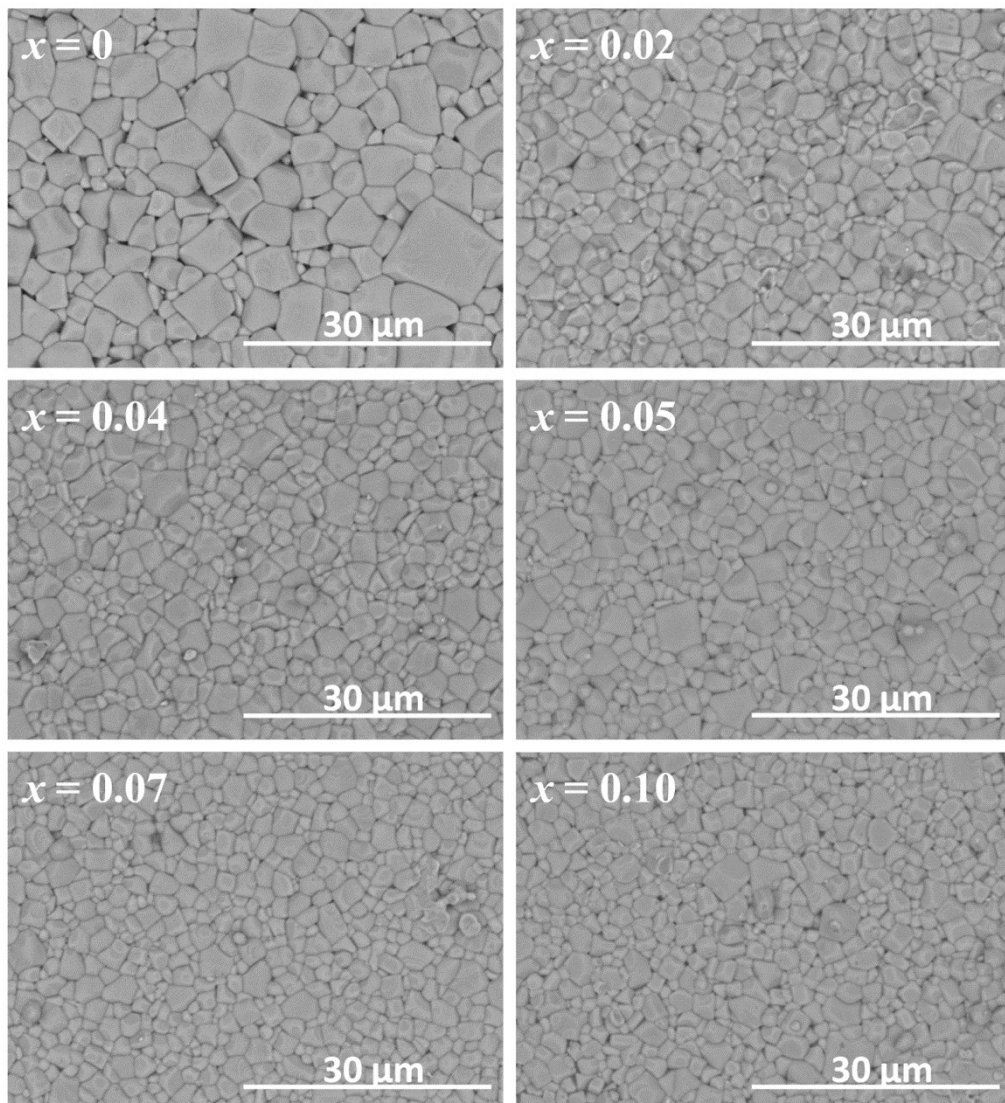


Fig. S1 SEM images for $(1-x)\text{AgNbO}_3-x\text{LiTaO}_3$ ceramics.

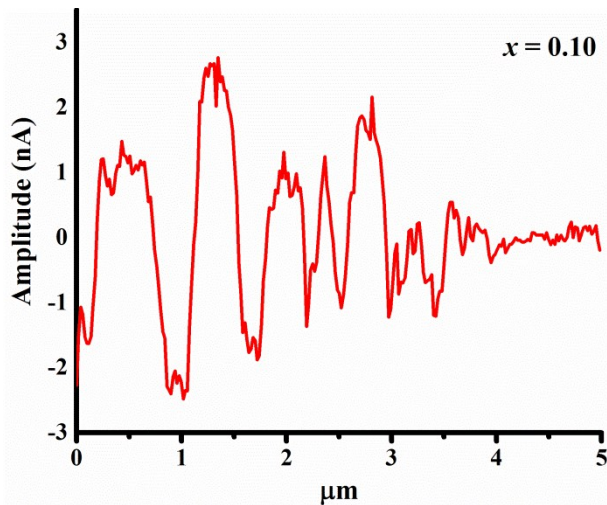


Fig. S2 Corresponding piezoresponse amplitude profiles generated from the line scan across the domains for the $0.9\text{AgNbO}_3\text{-}0.1\text{LiTaO}_3$ ceramic.

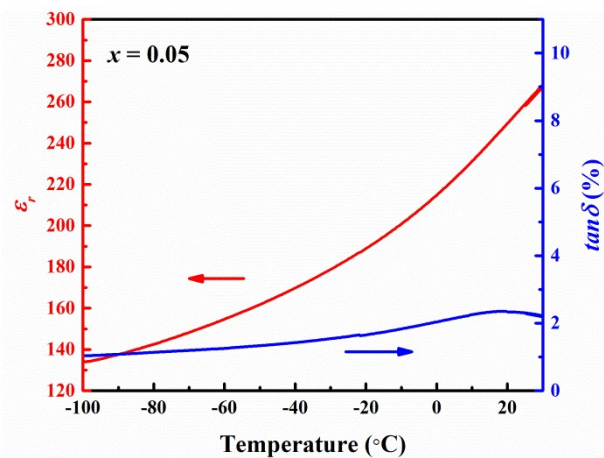


Fig. S3 Temperature dependence of the dielectric properties of the $0.95\text{AgNbO}_3\text{-}0.05\text{LiTaO}_3$ ceramic at low temperature.

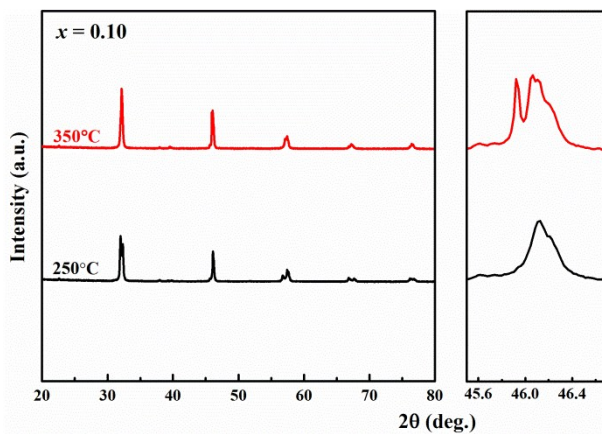


Fig. S4 Temperature dependent XRD patterns of the $0.90\text{AgNbO}_3\text{-}0.10\text{LiTaO}_3$ ceramic.

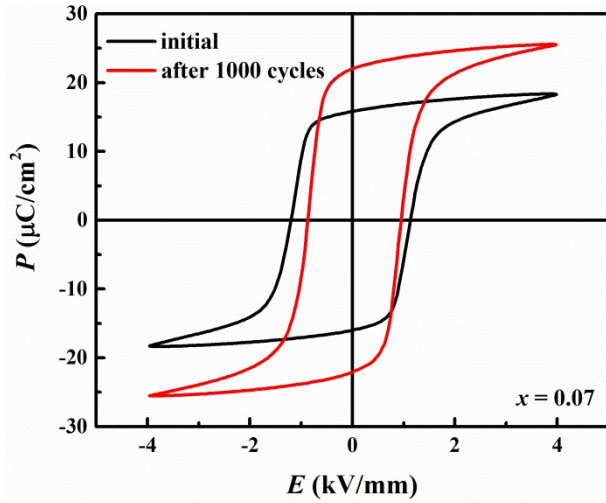


Fig. S5 Polarization-electric field (P - E) hysteresis loops of the $0.93\text{AgNbO}_3\text{-}0.07\text{LiTaO}_3$ ceramic with an increasing number of electric cycles.

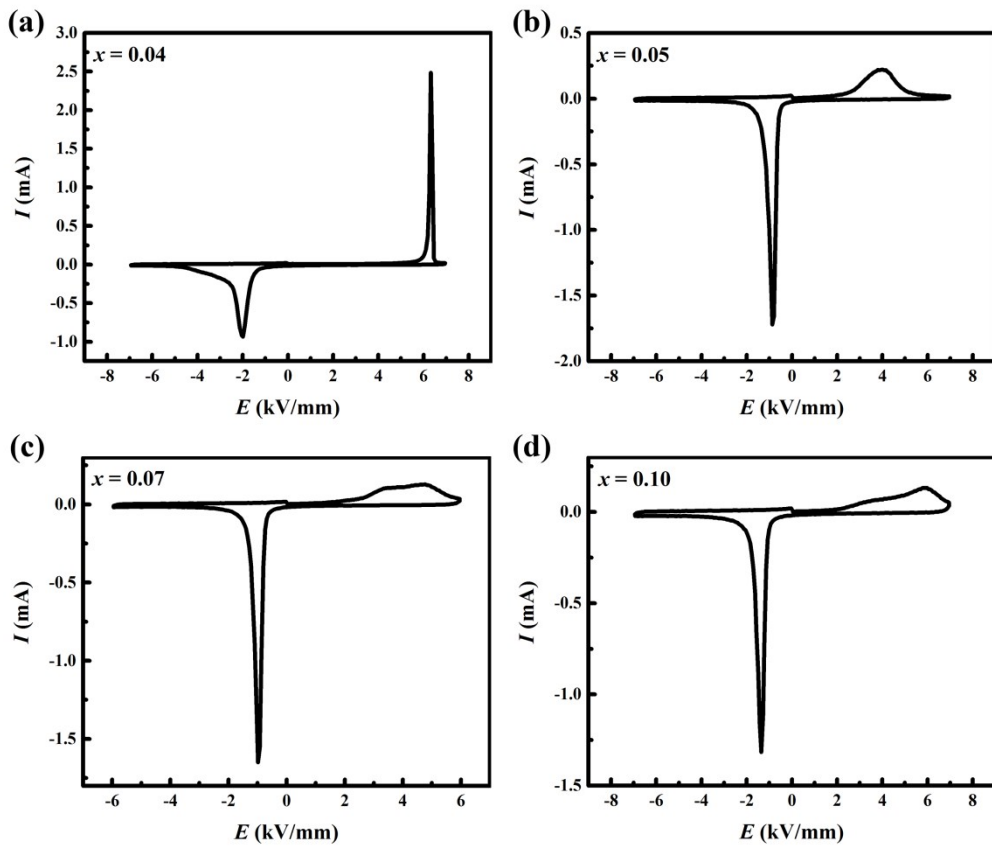


Fig. S6 First current-electric field (I - E) hysteresis loops of the fresh $(1-x)\text{AgNbO}_3\text{-}x\text{LiTaO}_3$ ceramics at room temperature.